

INFLUENCE OF INDIAN OCEAN WARMING ON THE SOUTHERN HEMISPHERE: ATMOSPHERE AND OCEAN CIRCULATION

K. Speer¹
C. Cassou²
M. Minvielle²

¹Oceanography, Florida State Univ., Tallahassee, FL, USA

²CERFACS, CNRS, Toulouse, France

1. Introduction

Observations of the atmosphere and ocean circulation in the southern hemisphere show significant trends over the past few decades (Kushner et al., 2001; Thompson and Solomon, 2002; Lu et al. 2004; Willis et al., 2004).

Greenhouse gases (GHG) have a direct effect on circulation through the radiative balance, while sea-surface temperature (SST) has an indirect effect, mainly from the tropics, through the modification of the Hadley Cell and associated Rossby wave teleconnections (Schneider et al., 2003; Hou, 1997; Jin and Hoskins, 1995).

Turner (2004) described the action of the tropical ENSO variability on Antarctica, especially the southeast Pacific Ocean and West Antarctic climate. He also noted the complexity of the indirect links and some inconsistency of the response at high latitudes, possibly a result of inadequately short records, but emphasized the effective control that tropical SST appears to exert on high-latitude climate.

In the northern hemisphere, Indian Ocean SST is thought to exert an influence on the trend of the wintertime annular mode

circulation (the Arctic Oscillation or AO; Bader and Latif, 2003). In the southern hemisphere, the Southern Annular Mode (SAM) represents the dominant mode of variability, and trends, or shifts, in the SAM also dominate overall trends in atmospheric circulation (Thompson and Solomon, 2002).

Fig. 1 shows the first two EOFs of NCEP June-August (JJA) sea-level pressure (SLP), along with time-series of amplitude. The first EOF (upper map) comprises nearly 60% of the variance and has a roughly annular form. Two additional curves are plotted along with the amplitude (in blue and red color). The first curve in black is the amplitude of the first EOF when ENSO is removed via a simple regression of SLP on the JJA nino4 index. [The two EOFs (with and without ENSO) are spatially very well correlated]. The second curve in green is an SST index computed over the entire Indian Ocean. We note that the trend of EOF 1 and the Indian Ocean SST index are very similar.

The second EOF shown in Fig 1 (lower map) shows a significant correlation with ENSO (green curve is the JJA nino4 index) that increases in later periods of the series.

While austral summer SAM variability is correlated with ENSO (L'Heureux and Thompson, 2006), this connection is much

¹ K. Speer, Dept. of Oceanography, FSU, Tallahassee, FL, 32303, USA; kspeer@ocean.fsu.edu

less significant in winter (Fig. 1a), and is mostly captured by the second mode of

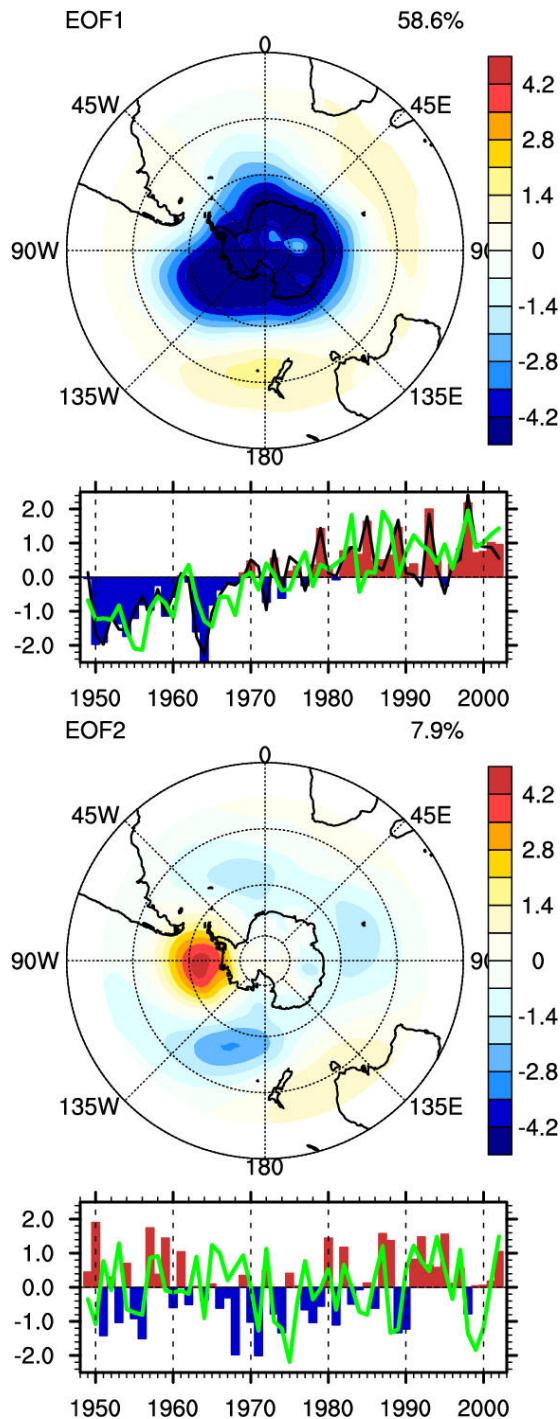


Figure 1: First two EOFs from NCEP SLP over the southern hemisphere. EOF 1 (upper, units of hPa), and time-series underneath (red/blue; EOF – ENSO in black – see text, Indian Ocean SST index in green). EOF 2 (lower) and time-series (red/blue;

variability of SLP (Fig.1b). Other tropical sources are expected to be important at that time of the year. Understanding the fundamental nature of these trends requires, we believe, some understanding of the role of tropical forcing independent of the ENSO signal.

Our intent in this study is to address the question of the role of tropical Indian Ocean SST forcing, independent of ENSO. Our premise is that this forcing is one of the primary agents driving large-scale trends in the atmosphere and ocean of the southern hemisphere.

The principal driving forces, SST anomalies and greenhouse gases, have been studied here with idealized forced atmospheric models and so-called GOGA-type experiments with or without evolving GHG. This sequence may be thought of as a way to attempt to distinguish the causes of trends in the evolution of the atmosphere due to trends in anthropogenically induced radiative forcing. Strong trends in southern hemisphere atmospheric circulation and climate have been attributed to forcing by the greenhouse gas ozone (Thompson and Solomon, 2002). We present here preliminary results of an investigation of the role of a warmer Indian Ocean sea surface temperature (SST) on the southern hemisphere circulation.

2. Atmosphere

For our first set of atmospheric forced runs we use the ARPEGE 4.3 model, with a resolution of $2.81^\circ \times 2.81^\circ$. This model is forced by repeated observed monthly varying SST climatology computed over 1950-2001, except for the Indian Ocean where in the first (second) simulation,

hereafter IBF (IAF), the 1950-1976 (1977-2001) mean state is applied.

The mean winter JJA SLP difference between the two runs shows a strong signal in the southern hemisphere (Fig. 2) in response to the Indian Ocean warming. The latter is associated with intensified local convection and upward motion thus altering the local Hadley Cell in the eastern part of the basin. The subtropical jet is accordingly modified between 90°-180°E as well as the Rossby wave activity in the southwestern Pacific sector. This leads downstream to a wave-train structure characterized by anomalous highs between Australia and New Zealand and deeper lows especially in the Ross Sea region 160°W. The anomalous high reappears farther east closer to the Antarctic Peninsula, creating a sign reversal across the peninsula.

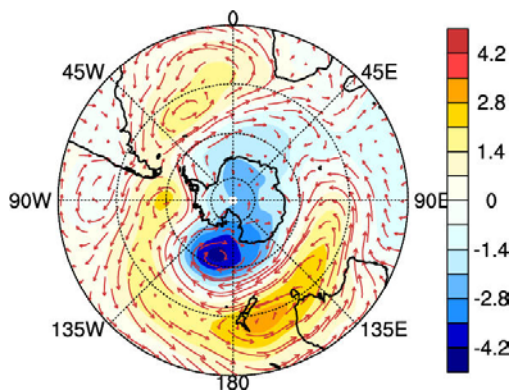


Figure 2: Mean winter (JJA) SLP difference between the two simulations.

These SLP differences are consistent with a stronger anticyclone over the South Atlantic and the western South Pacific, extending westward into the southern Indian Ocean. A stronger flow of warmer air toward the Antarctic continent occurs in the Amundsen Sea between the Antarctic Peninsula and the Ross Sea, and

in the southern Indian Ocean near the Kerguelen Islands.

A comparison between this difference and observed SLP trends derived from NCEP (Fig.1), which are dominated by trends in the first, roughly annular mode, shows a similar latitudinal structure. The zonal structure arising from regional Indian Ocean SST forcing is much more evident in the model differences. These mean SLP results are used in the following section to determine the ocean response to a warmer Indian Ocean.

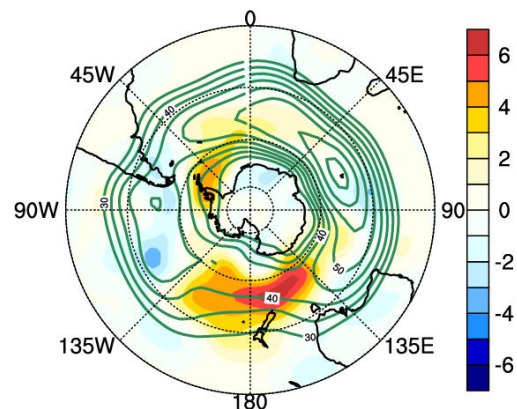


Figure 3: Standard deviation (m) of bandpassed (2.5-8 day) 500hPa surface and climatological storm track (green contours from 5-30m) showing enhanced activity.

To illustrate storm activity, high-frequency (2.5-8d period) variance was calculated in the two runs (Fig. 3). The result shows an enhanced storm activity consistent with an eastward shift of the maximum in activity and zonal extension of the maximum south of Australia and New Zealand. Atmospheric eddies are found from more specific diagnostics (not shown) to play a significant role in setting and maintaining the atmospheric model response.

Finally, we calculated the first EOF from each of the 20 yr IBF (early period) and IAF (later warmer period) runs to examine

the dominant change in variability (Fig. 4). Both cases show a SAM-like 1st mode, but the center of action in the loading pattern has shifted toward the southeast Pacific and Antarctic Peninsula after warming. The significance of these changes was investigated by removing some years and they appear robust; however, they must be interpreted cautiously at this stage because of the small sample size.

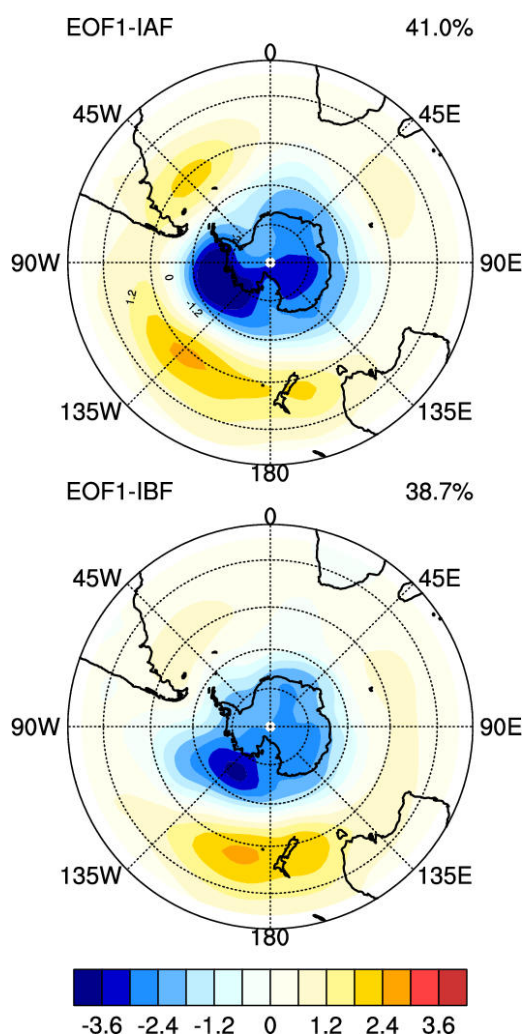


Figure 4: First EOF for more recent warm SST (IAF; upper) and for early period (IBF; lower).

3. Ocean

In this section we present the South Pacific Ocean gyre response to the mean SLP trend forced by warming in the Indian Ocean. To determine this response, an idealized ocean general circulation model was forced by the mean winds from IBF and from IAF. The model was configured with a single homogenous layer, flat-bottomed, in two ocean basin geometries. The first was a South Pacific geometry (Fig. 5) and the second was a circumpolar Southern Ocean geometry (Fig. 6). The model was spun up to a steady state, with a lateral frictional balance between forcing and dissipation. Further modeling will include realistic stratification, bathymetry, and time-dependent forcing by all (stress, heat, water) air-sea fluxes.

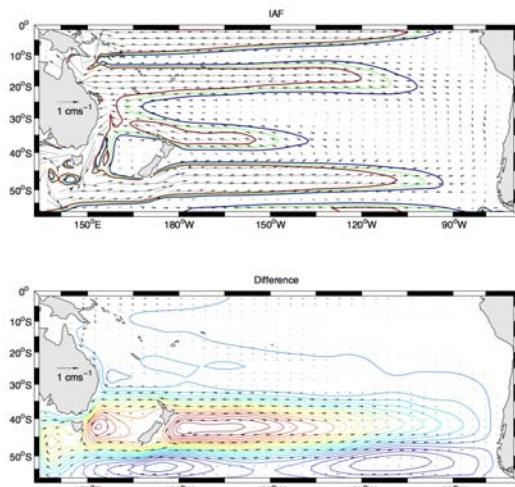


Figure 5: South Pacific Ocean simulation. Upper panel: velocity with speed contours [4,5,6 mm/s]; Lower panel, Sea-surface height; maximum Δ SSH=4.5 cm, showing the strengthening of the S. Pacific gyre.

The main response of the South Pacific Ocean to Indian Ocean warming is an increase in strength of the subtropical gyre, associated with an increase in sea

level (Fig. 5). The model is too idealized to compare directly the sea level (or sea-surface height, SSH) change, equivalent to a few centimeters of sea-level height increase; however, the pattern of the increase is roughly consistent with trends in SSH determined from satellite altimetric observations (AVISO). A decrease in sea level in the southeast Pacific near 120W is also qualitatively consistent, but the decrease farther west, near 170 E is not clearly associated with observed trends. Given the flat bottom and artificial southern and western boundaries of this configuration, only a rough agreement could be expected.

To illustrate the pattern on a larger domain, the full Southern Ocean was also configured, again with a flat bottom (Fig. 6). The response also shows the SSH increase in the subtropical South Pacific, as well as a weaker increase in the Indian Ocean gyre and Agulhas Current. Circulation in the ACC has decreased somewhat, by 3% or so, and the associated meridional SSH gradient is reduced. Thus SSH is lower on the northern side and higher on the southern side of the ACC. Although there is some observational evidence for a band of reduced sea level on the northern side of the ACC, with centers southeast of Africa and southeast of Australia, these results are more difficult to compare directly with observed trends because of the absence of topography. At this stage they mainly provide a reference for further simulations. The results also suggest that the response of the idealized ACC to IO warming is not acceleration but a deceleration.

Roemmich et al. (2006) found an increase in the strength of the Pacific subtropical gyre based on a variety of observations, showing that the changes are associated

with a deepening of the entire ocean thermocline, to 1800m depth or so. Dynamic height changes below a depth of 200m were about 5cm, with a pattern consistent with SSH trends from satellite altimetry. Qiu and Chen (2006) used trends from NCEP winds to determine changes in the South Pacific gyre. Our results are consistent, qualitatively, with these observations and model results.

Roemmich et al. (2006) attributed the gyre changes to changes in the wind, specifically to changes in the SAM, but the changes in wind field are better described as long-term trends in the atmosphere that project onto a SAM-like pattern. The key issue is the causes of these trends, and our results suggest that warmer SST in the tropical Indian Ocean generates a significant fraction of the observed changes in the South Pacific.

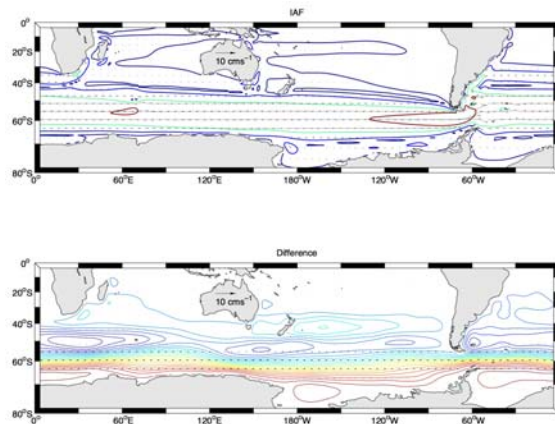


Figure 6: Southern Ocean simulation. Upper panel: velocity with speed contours [0.4, 2,7,14.5 cm/s]; Lower panel: Sea-surface height; maximum Δ SSH=7.7 cm, showing the weakening of the ACC.

We can interpret the 1st mode of the variability from IAF (Fig. 4) as the new SAM for the warmer state, and we do find important changes in this pattern of variability of possible significance to the

ocean. In particular, significant change appears to take place between the West Antarctic Peninsula and the Ross Sea. The SAM is more intense after warming, which could lead to stronger variability in upwelling and ice melt in this region.

4. Direct versus indirect effect

Ensemble atmospheric model runs were performed with ARPEGE to investigate the response with fixed and evolving greenhouse gases. In all cases in these runs (commonly referred to as GOGA runs) the observed monthly varying SST was prescribed in all oceanic basins.

Results suggest that the GHG effect strongly projects onto the SAM, and that the case without GHG, which includes indirect SST forcing from all ocean basins, shows less resemblance to the observed trends in SLP from NCEP. These results, and potential nonlinear feedbacks with tropical SST (Hartmann et al, 2000), are currently under investigation.

5. Conclusions

We have found that higher SST in the tropical Indian Ocean has an important effect on the atmospheric circulation and wind-forced ocean circulation in idealized models. The inferred changes are consistent with some observed trends, and plausibly explain a significant fraction of these trends.

Additional model runs support previous conclusions about the role of GHG on the atmospheric circulation and are needed to help distinguish direct and indirect forcing mechanisms for climate change, and to evaluate quantitatively the relative role of these effects.

6. References

AVISO. <http://www.aviso.oceanobs.com>

Hartmann, D. L., J. M. Wallace, V. Limpasuvan, D. W. J. Thompson, and J. R. Holton (2000) Can ozone depletion and global warming interact to produce rapid climate change? *Proc. Nat. Acad. Science* 97: 1412-1417.

Jin, F.F., and B.J. Hoskins (1995) The direct response to tropical heating in a baroclinic atmosphere. *J. Atmos. Sciences*, 52: 307-319.

Kushner, P.J., I. M. Held, and T.L. Delworth (2001) Southern hemisphere atmospheric circulation response to global warming. *J. Climate*, 14:2238-2249.

Lu, J., R.J. Greatbatch, and K.A. Peterson (2004) Trend in northern hemisphere winter atmospheric circulation during the last half of the 20th Century. *J. Climate*, 17: 3745-3760.

Marshall, G. J., 2002: Trends in Antarctic geopotential height and temperature: A comparison between radiosonde and NCEP-NCAR reanalysis data. *J. Clim.*, 15, 659-674.

Marshall, G. J., 2003: Trends in the southern annular mode from observations and reanalyses. *J. Clim.*, 16, 4134-4143.
L'Heureux, M. L., D. Thompson (2006) Observed Relationships between the El Niño–Southern Oscillation and the Extratropical Zonal-Mean Circulation, *J. Climate*, 19: 276-287.

Qiu, B. and S. Chen (2006) Decadal variability in the large-scale sea surface height field of the South Pacific Ocean:

observations and causes. *J. Phys. Ocean.*,
in press.

Renwick, J. A., 2004: Trends in the Southern Hemisphere polar vortex in NCEP and ECMWF reanalyses. *Geophys. Res. Lett.*, 31, L07209, doi:10.1029/2003GL019302.

Roemmich, D., J. Gilson, R. Davis, P. Sutton, S. Wjiffels, and S. Riser (2006) Decadal spin-up of the South Pacific subtropical gyre. *J. Phys. Ocean.*, in press.

Schneider, E. K., L. Bengtsson, and Z. Hu (2003) Forcing of the northern hemisphere climate trends. *J. Atmos. Sciences*, 60: 1504-1521.

Shindell, D. T. and G. A. Schmidt, 2004: Southern Hemisphere climate response to ozone changes and greenhouse gas increases. *Geophys. Res. Lett.*, 31, L18209, doi:10.1029/2004GL020724.

Thompson, D.W.J., and S. Solomon (2002) Interpretation of recent southern hemisphere climate change. *Science* 296: 895-899. DOI: 10.1126/science.1069270.

Turner, J. (2004) The El Niño-southern oscillation and Antarctica. *International J. of Climatology*, Vol. 24: 1 – 31.

Willis, J.,K., D. Roemmich, and B. Cornuelle (2004) Interannual variability in upper ocean heat content, temperature, and thermosteric expansion on global scales. *J. Geophys. Res.* 109, C12036, doi:10.1029/2003JC02260.